Water Splitting

International Edition: DOI: 10.1002/anie.201412389
German Edition: DOI: 10.1002/ange.201412389

Fast and Simple Preparation of Iron-Based Thin Films as Highly Efficient Water-Oxidation Catalysts in Neutral Aqueous Solution**

*Yizhen Wu, Mingxing Chen, Yongzhen Han, Hongxia Luo, Xiaojun Su, Ming-Tian Zhang, Xiaohuan Lin, Junliang Sun, Lei Wang, Liang Deng, Wei Zhang, and Rui Cao**

Abstract: *Water oxidation is the key step in natural and artificial photosynthesis for solar-energy conversion. As this process is thermodynamically unfavorable and is challenging from a kinetic point of view, the development of highly efficient catalysts with low energy cost is a subject of fundamental significance. Herein, we report on iron-based films as highly efficient water-oxidation catalysts. The films can be quickly deposited onto electrodes from Fe^{II} ions in acetate buffer at pH 7.0 by simple cyclic voltammetry. The extremely low iron loading on the electrodes is critical for improved atom efficiency for catalysis. Our results showed that this film could catalyze water oxidation in neutral phosphate solution with a turnover frequency (TOF) of 756 h^{-1} at an applied overpotential of 530 mV. The significance of this approach includes the use of earth-abundant iron, the fast and simple method for catalyst preparation, the low catalyst loading, and the large TOF for O_2 evolution in neutral aqueous media.*

Catalytic water splitting is an appealing way of using solar energy to produce hydrogen fuels as a clean, carbon-free, and renewable energy source and thus to eliminate the energy and environmental problems caused by burning fossil fuels.[1–3] Electrochemical water splitting has received extensive attention because this process can convert electric energy from renewable but intermittent sources into chemical energy for easier storage and delivery.[4–6] As one of the half reactions, water oxidation becomes the bottleneck for large-scale water splitting, as it is challenging from both thermodynamic and kinetic points of view.[1,7] Extensive efforts have been made to develop efficient and robust water-oxidation catalysts (WOCs) that can catalyze oxygen evolution at considerable rates at low overpotentials (η). Examples include homogeneous and heterogeneous systems based on noble metals, such as Ru[8–10] and Ir,[10–12] and first-row transition metals, such as V,[13] Mn,[14–20] Fe,[21–25] Co,[2,26–30] Ni,[4,6,31,32] and Cu,[5,33,34] and mixed-metal materials.[35–39] However, substantial improvement of catalyst activity and stability is still needed, in particular for WOCs made of cheap earth-abundant transition-metal elements.

Iron is the most abundant transition metal in the earth's crust, and it is less toxic than Co and Ni. Meanwhile, iron is attractive for water oxidation because of its rich redox properties and the extensive biological/biomimetic activity of iron enzymes/complexes for oxygen activation.[40,41] Iron-based films have been much less explored as electrocatalysts for water oxidation than those of Co and Ni, although iron oxides (Fe_2O_3) have been shown to be photocatalysts for this process[22,23] and are known to be important cocatalysts for Co and Ni oxides.[35,36,38,39] One possible reason is that the direct preparation of iron-based films by electrodeposition, a method generally employed to deposit other metal oxides onto electrodes, is difficult because Fe^{III} ions will precipitate out (probably as $Fe(OH)_3$, $K_{sp} = 2.6 \times 10^{-39}$) from water under neutral conditions.

Herein, we report an iron-based thin film as a highly efficient catalyst for water oxidation under neutral conditions. This iron-based thin film was prepared in a fast and simple manner through electrodeposition from a solution of Fe^{II} ions in acetate buffer at pH 7.0. Characterization of the resultant film revealed that it had a very low iron coverage (10.2 nmol cm^{-2}) on the electrode and was composed of iron-based polycrystalline particles of approximately 5 nm in size. This film could catalyze the electrochemical oxidation of water to O_2 in neutral, iron-free phosphate solution with a turnover frequency (TOF) of 756 h^{-1} at $\eta = 530$ mV. The low catalyst loading and high TOF of this iron-based film for water oxidation are significant and will contribute to the future development of iron-based WOCs.

Iron-based films were initially prepared by electrodeposition on glassy carbon (GC) electrodes. Prior to the

[*] Y. Z. Wu,[+] M. X. Chen,[+] Y. Z. Han,[+] Prof. Dr. H. X. Luo, Prof. Dr. R. Cao
Department of Chemistry, Renmin University of China
Beijing 100872 (China)
E-mail: ruicao@ruc.edu.cn
X. J. Su, Prof. Dr. M.-T. Zhang
Center of Basic Molecular Science (CBMS)
Department of Chemistry, Tsinghua University
Beijing 100084 (China)
X. H. Lin, Prof. Dr. J. L. Sun
College of Chemistry and Molecular Engineering
Peking University
Beijing 100871 (China)
L. Wang, Prof. Dr. L. Deng
State Key Laboratory of Organometallic Chemistry, Shanghai Institute of Organic Chemistry, Chinese Academy of Sciences
Shanghai 200032 (China)
Prof. Dr. W. Zhang, Prof. Dr. R. Cao
School of Chemistry and Chemical Engineering
Shaanxi Normal University
Xi'an 710119 (China)
[+] These authors contributed equally to this work.

[**] We are grateful for support from the "Thousand Talents Program" of China, the National Natural Science Foundation of China under grant no. 21101170, the Fundamental Research Funds for the Central Universities, and the Research Funds of Renmin University of China.
Supporting information for this article is available on the WWW under http://dx.doi.org/10.1002/anie.201412389.

dissolution of iron(II) sulfate, nitrogen gas was bubbled vigorously through an acetate buffer (pH 7.0) for at least 30 min to remove oxygen in the solution and thus prevent the oxidation of Fe^{II} to Fe^{III} and enable well-controlled deposition to occur. At pH 7.0, Fe^{III} will precipitate, which may hinder efficient electron transfer on the electrode surface and may also affect the composition and arrangement of deposited films. A cyclic voltammogram (CV) recorded on a GC electrode for $FeSO_4$ (1.0 mM) in 0.1 M sodium acetate buffer (pH 7.0) displayed an anodic wave at $E_{p,a} = 1.20$ V versus the normal hydrogen electrode (NHE; all potentials reported herein are referenced to NHE). Unless otherwise noted, compensated cell resistance (iR) was measured prior to cyclic voltammetry. At more positive potentials, a pronounced catalytic wave appeared with an onset at about 1.30 V (Figure 1a). In blank controls, there were no such anodic waves in the acetate buffer alone. In successive CVs, the first anodic wave moved cathodically to 1.13 V (see Figure S1 in the Supporting Information), probably because of the instability of the electrode at the very start and the rearrangement of deposited materials on the electrode surface. The second catalytic wave showed a similar cathodic shift accompanied by a slight current increase.

After electrodeposition in one CV cycle (0.20–1.35 V, Figure 1a), the GC electrode was removed from the acetate buffer, gently rinsed with deionized water, and then immersed in (iron-free) 0.1 M phosphate buffer solution at pH 7.0. When this pretreated GC electrode was used, a strong catalytic wave of 10.1 mA cm^{-2} with an onset potential of 1.30 V was observed by cyclic voltammetry (at $j = 1.0$ mA cm^{-2}; Figure 1b). This result confirms the formation of a highly active WOC film on the GC electrode. The activity of this film in neutral aqueous solution is remarkable, as basic media are typically required for water oxidation with many metal-oxide-based materials.[4,6,32,36–38]

Subsequently, we produced iron-based films under various conditions and examined their performance for water oxidation. First, we deposited films on GC electrodes by CV scanning to more positive potentials. A film generated in one CV cycle of 0.20–1.55 V (Figure 1b) showed very similar electrochemical behavior to that of the film formed during one CV cycle of 0.20–1.35 V, thus indicating that larger anodic potentials applied for film deposition by cyclic voltammetry have a negligible effect on catalysis. This result is significant for large-scale preparation and application, as it is critical to make active films with less energy input. Next, we examined films generated by cyclic voltammetry with various scan rates and found that they showed similar catalytic waves, although earlier onsets and slightly increased currents were observed for films formed at lower scan rates (see Figure S2). It has been shown that the morphology and arrangement of metal-oxide films deposited on electrodes depend on the CV scan rate.[42,43] We also found that at lower scan rates, more of the catalyst was deposited with a more compact arrangement (see below for details). As a result, in films formed by cyclic voltammetry at lower scan rates, more iron active sites were generated for catalysis. Finally, we found that films deposited in five CV cycles displayed an enhanced catalytic current (11.2 mA cm^{-2}) and an earlier onset (1.27 V, measured at $j =$ 1.0 mA cm^{-2}) as compared to films prepared in one CV cycle (see Figure S3). This difference is attributed to the larger catalyst loading derived from more CV cycles.[44] The current declined as the applied potential increased above 1.45 V (Figure 1b), which indicated the exfoliation of the catalyst film from GC electrodes under conditions for oxygen evolution. This hypothesis was verified by successive CV cycles, which showed a constant decrease in the current as the number of CV scans increased (see Figure S16).

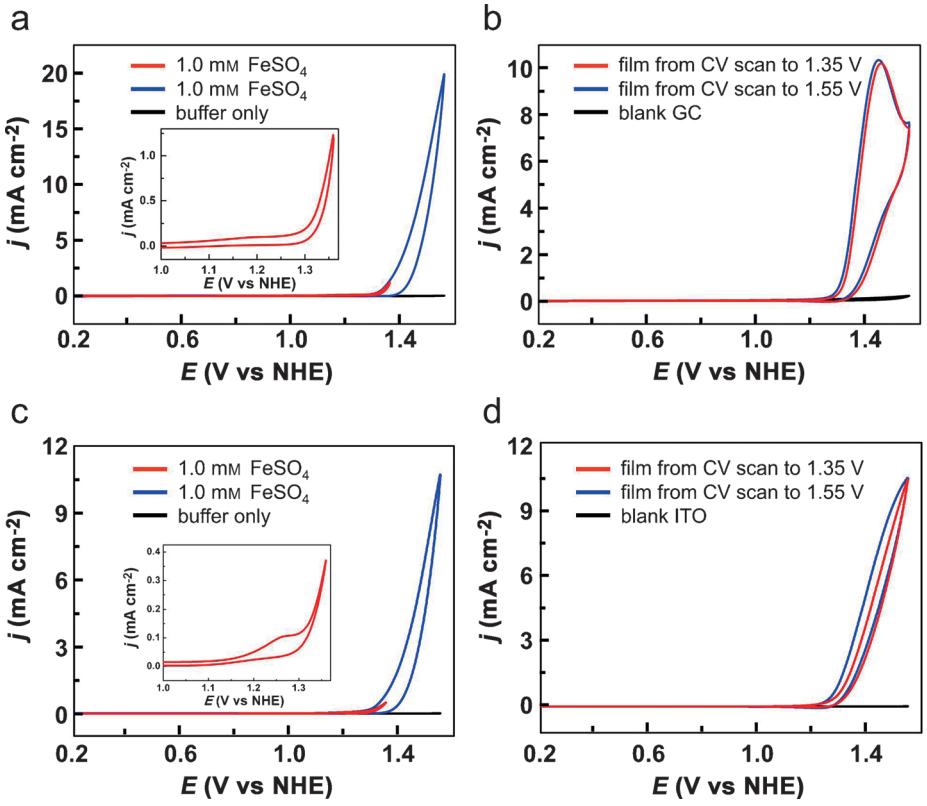

Figure 1. a,c) CVs of GC (a) and ITO electrodes (c) in 0.1 M acetate buffer (pH 7.0) with and without $FeSO_4$ (1.0 mM). Inserts: Magnification of the CV scans to 1.35 V. b,d) CVs of blank and catalyst-coated GC (b) and ITO electrodes (d) in (iron-free) 0.1 M phosphate buffer (pH 7.0; scan rate: 50 mV s^{-1}, 20 °C).

Similar results were obtained when indium tin oxide (ITO) electrodes were used to prepare this iron-based film (Figure 1c). An ITO electrode with a catalyst film deposited in one CV cycle of 0.20–1.35 V displayed a catalytic current of 10.5 mA cm^{-2} at 1.55 V, and a value of $\eta = 480$ mV was determined at the potential with the current density $j =$ 1.0 mA cm^{-2} (Figure 1d). The influences of the applied anodic potential, the scan rate, and the number of CV cycles for film generation and deposition on ITO electrodes were investigated. The amount of deposited iron increased if the scan rate decreased, increased slightly upon CV scanning to more positive potentials, and increased considerably with more CV cycles (see Table S2 in the Supporting Information). On the basis of our results, and also in consideration of the time and energy cost, we chose five CV cycles of 0.20–1.35 V at a scan rate of 50 mV s^{-1} in the following experiments to make the iron-based films, unless otherwise noted. As compared to those on GC electrodes, catalyst films on ITO exhibited much enhanced stability (see Figure S17; the same catalytic activities were observed in successive CV cycles). Therefore, ITO electrodes were used in all studies to determine the film morphology and composition, the Faradaic efficiency of the catalyst for O_2 evolution, the catalyst stability, and the Tafel plot of the catalyst.

The morphology and composition of the catalyst films were analyzed. Scanning electron microscopy (SEM) and energy-dispersive X-ray (EDX) analysis of ITO electrodes before and after electrodeposition clearly showed the formation of an iron-based film on the ITO surface (see Figures S4 and S5). These SEM images revealed that more-compact films were formed at lower scan rates. Transmission electron microscopy (TEM) of the material scraped from the ITO electrode after film deposition exhibited layered structures (Figure 2a,b), and high-resolution TEM (HRTEM) showed that it was composed of aggregates of polycrystalline particles of approximately 5 nm in size (Figure 2c,d). The poorly defined diffraction rings in the SAED pattern (Figure 2a, insert) and the distorted lattice observed in the HRTEM images indicated the poor crystallinity of the deposited material on the electrode. The deposition of iron-based materials was further verified by X-ray photoelectron spectroscopy (XPS; see Figure S7). The XPS spectrum of the Fe 2p energy region could be reasonably well resolved to show the characteristic peaks of Fe^{III} (Figure 2e). The energy separation between the envelope (710.8 eV) and satellite (719.1 eV) of Fe $2p_{3/2}$ was 8.3 eV. This value is consistent with the Fe^{III} oxidation state and is different to the value for Fe^{II}, which lies around 5 eV. The envelope of Fe $2p_{3/2}$ can be fitted well on the basis of the multiplets and surface peak for Fe^{III} $2p_{3/2}$.[45,46] The Fe^{III} valence state was also examined by Mössbauer spectroscopy (see Figure S9 and Table S1). Analysis of the Mössbauer data suggested the existence of iron in two different kinds of coordination environments with an approximate ratio of 44:56. The isomer-shift values of approximately 0.38 suggested that both are Fe^{III} states.[47,48] The XPS spectrum of the O 1s energy region could be resolved with three strong subpeaks (Figure 2f), which suggested that this iron-based film is distinct from the amorphous FeOOH WOC material recently reported by Mullins and co-workers.[49] The lower-binding-energy (BE) peaks at 530.0 and 531.4 eV can be assigned to oxygen atoms of oxide ions and hydroxy groups, respectively. The higher-BE peak at 532.4 eV is characteristic of carbonyl oxygen atoms.

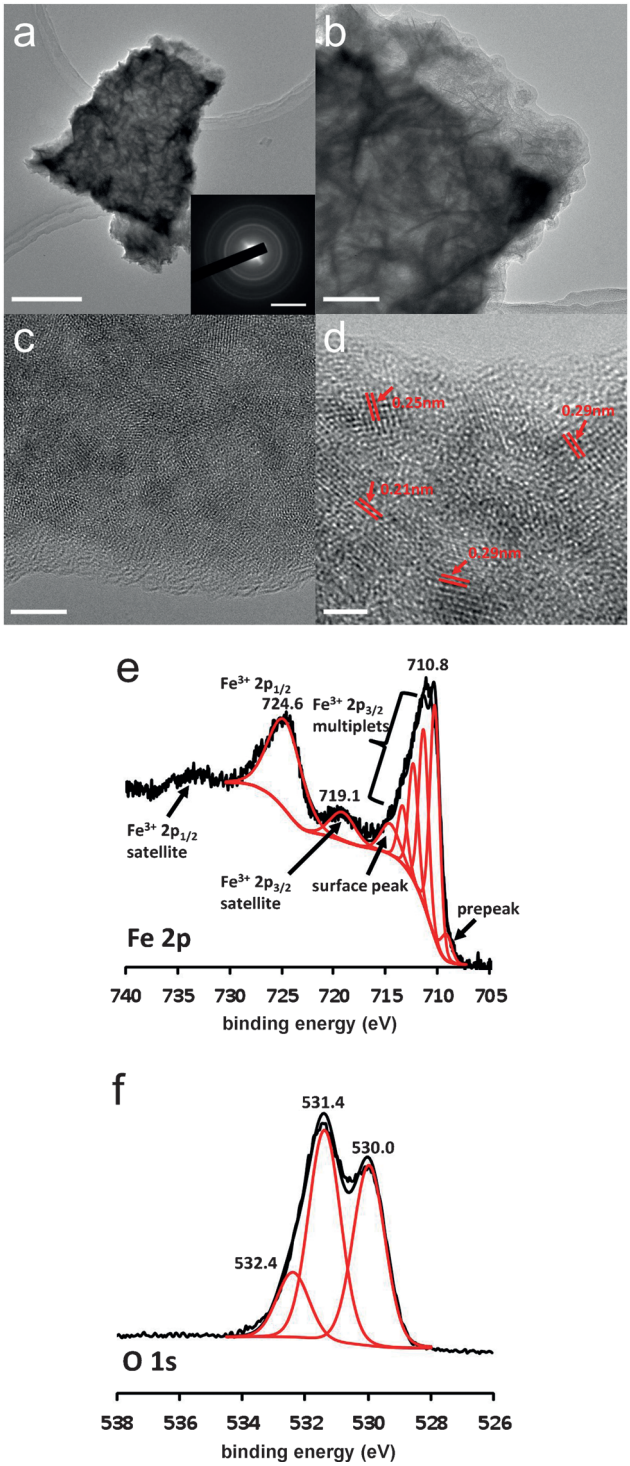

Figure 2. a, b) TEM and c, d) HRTEM images of a sample of the as-prepared iron-based film scraped from the ITO electrode. The insert in image (a) is the selected-area electron diffraction pattern (SAED) of the aggregates. Scale bars: a) 500 nm (insert, 5 nm^{-1}); b) 100 nm; c) 5 nm; d) 2 nm. e, f) Sections of the XPS spectrum around the Fe 2p (e) and O 1s (f) energy regions.

This result is indicative of the presence of acetate groups in the film.[50] Likewise, the XPS spectrum of the C 1s region showed a strong peak at 288.4 eV, which is consistent with acetate groups in the deposited film (see Figure S8).[50] Infrared spectroscopy further confirmed the acetate content by showing strong resonance peaks for both carboxy and methyl groups (see Figure S6).

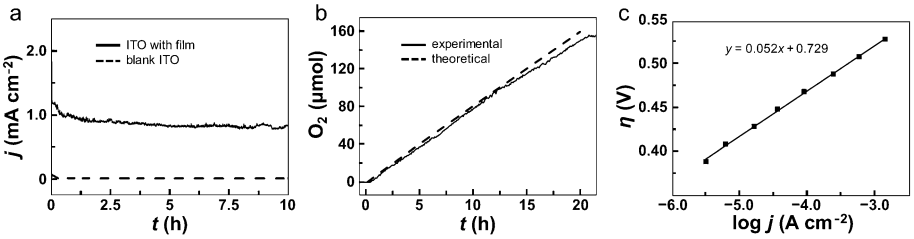

Figure 3. a) Current curves of blank and catalyst-coated ITO during CPE. b) Observed and theoretical amount of O_2 evolved during CPE for 20 h with catalyst-coated ITO. Conditions: 0.1 M phosphate buffer (pH 7.0), applied potential: 1.35 V, $S = 1.0\ cm^2$, 20 °C. c) Tafel plot, $\eta = E_{appl} - iR - E_0$, of the iron-based film in 0.1 M phosphate buffer (pH 7.0). In the equation, E_{appl} is the applied potential, and $E_0 = 0.82$ V is the thermodynamic potential for water oxidation at pH 7.0. The slope of the graph is 52 mV per decade.

To determine the surface iron-catalyst coverage on the electrode, we dissolved iron-based films generated in five CV cycles on 17.5 cm^2 ITO in 0.1M HNO_3 (5.0 mL) and subjected the resultant solution to inductively coupled plasma atomic emission spectroscopy (ICP-AES). The number of deposited iron atoms could be calculated by the working-curve method. Our results showed that an amount of 10.2 nmol of iron was electrodeposited onto 1.0 cm^2 of the ITO electrode, which corresponds to 15 iron atoms per 25 $Å^2$. This number indicates the formation of a three-atom-layer film in five cycles of CV experiments.[4] Furthermore, the integrated charges that passed through the electrode gave a surface iron coverage of (11.0 ± 0.5) nmol per 1.0 cm^2, which is in a good agreement with the result derived from ICP-AES, as only a portion of the charge was consumed for electrodeposition (i.e. the rest was consumed for water oxidation). Owing to the extremely low catalyst loading, the iron-based films were transparent (see Figure S10). This transparence could be crucial for the application of film catalysts in light-harvesting devices for water splitting.[51]

The catalyst-loaded ITO electrode was applied to controlled-potential electrolysis (CPE). By the use of a two-compartment cell, electrolysis was carried out in a 0.1M phosphate buffer (pH 7.0) at 1.35 V. During CPE, a stable current density of approximately 0.90 $mA\,cm^{-2}$ was maintained (Figure 3a), which was indicative of the stability of the catalyst film. The slight decrease in the current was caused by a decrease in the pH value during electrolysis. After CPE for a period of 10 h, the measured pH value was 6.75. If the pH value was adjusted back to 7.0, the current for CPE could be recovered. Furthermore, after CPE for 10 h, the ITO electrode displayed an almost identical CV to that before CPE (see Figure S11). The small diminution may be attributed to the exfoliation of the catalyst (see Table S2). In control experiments with blank ITO electrodes, the current was at a baseline level of $< 30\ \mu A\,cm^{-2}$. During CPE with catalyst-loaded ITO, a substantial amount of bubbles of O_2 gas were observed, which confirmed that the electrocatalytic current corresponded to water oxidation to produce O_2. The amount of evolved O_2 was measured by a calibrated Ocean Optics FOXY probe (model NeoFox). During electrolysis for 20 h, 61 coulombs of charge passed (see Figure S12) with 156 μmol of O_2 evolved (Figure 3b), which gave a Faradaic yield of more than 98%. At 1.35 V and pH 7.0, the turnover number (TON) of this iron-based film was 1.5×10^4, and the turnover frequency (TOF) was 756 h^{-1} per deposited Fe ion. This result is extraordinary: The TOF value of this iron-based film is one to two magnitudes larger than the TOF values of many well-known catalyst films of Mn, Co, and Ni at the same or even higher overpotentials (Table 1).[2,4,15–20,27,28,32,52]

As metal phosphates are known as WOCs, we examined the possibility that the high activity of the iron-based film was due to the formation of an iron–phosphate-based film as the active material. The surface Fe/P atomic ratio of the catalyst film after CPE in a phosphate buffer was quantified by XPS to be 0.92:0.08 (see Figure S18).[53] The Fe $2p_{3/2}$ XPS peak after

Table 1: Comparison of catalytic performances and conditions for a variety of WOC films containing earth-abundant transition metals.

Film	Catalyst loading [$nmol\,cm^{-2}$]	pH	η [mV at $j = 1\ mA\,cm^{-2}$]	TOF [h^{-1} at $\eta = 530$ mV]	Ref.
Fe-based	10.2	7.0	480	756	this study
Mn-based	80	7.0	590	36	[15]
nano-MnO_2	–[a]	7.0	–[a]	0.18 (600 mV)	[52]
α-MnO_2-Py	≈1600	7.5	660	11.3 (910 mV)	[16]
$Mn_3(PO_4)_2$	611	7.0	680 (0.32 $mA\,cm^{-2}$)	4.4 (680 mV)	[17]
$LiMnP_2O_7$	1059	7.0	680 (0.5 $mA\,cm^{-2}$)	4.2 (680 mV)	[18]
PAH-MnO_2	1300	8.0	590 (0.03 $mA\,cm^{-2}$)	–[a]	[19]
MnO_x-573 K	1800	7.0	450	–[a]	[20]
Co-based	100	7.0	550	61.2	[2,15] and this study[b]
Co-based	1000	7.0	–[a]	10 (545 mV)	[27]
$Li_2Co_2O_4$	276	7.2	545	8.5 (580 mV)	[28]
Ni-based	100	9.2	540	36	[4,15] and this study[b]
NiO_x-en	270	9.2	510	54 (ca. 610 mV)	[32]
NiO_x-aqua	280	9.2	570	39.6 (ca. 610 mV)	[32]
NiO_x-NH_3	290	9.2	560	–[a]	[32]

[a] Not reported. [b] The cobalt/nickel-based films were prepared according to Refs. [2] and [4]. The performance of these two catalyst films was examined by us and others (see Ref. [15]).

CPE could be well resolved on the basis of the Fe^{III} subpeaks, and the locations and shapes of these subpeaks were identical to those before electrolysis (see Figure S19). Furthermore, the Fe $2p_{3/2}$ peak position (710.8 eV) of our samples before and after electrolysis was 1.7 eV lower than the Fe $2p_{3/2}$ peak position of iron phosphate (ca. 712.5 eV[54,55]). Considering this large difference and the very low phosphorus content in the sample after electrolysis, we assumed that the small amount of phosphorus was due to the physical adsorption of phosphate on the electrode surface, and that it contributed negligibly to water oxidation. An additional argument against the possibility that an iron–phosphate-based film was formed and acted as the active material for water oxidation is that the catalytic current did not increase during successive CV cycles (see Figure S17) or during CPE (Figure 3a).

There are several lines of evidence to support the stability of this catalyst film. First, the current remained constant during electrolysis for 10 h at 1.35 V, and the electric charges accumulated had a linear dependence on time (see Figure S12). Second, the CV of the film after CPE was almost identical to that before electrolysis (see Figure S11). Third, the CV of an aged film (in air for 24 h) was the same as that of a freshly prepared film (see Figure S13). However, the catalyst film was less stable during CPE at higher applied potentials. For example, at a potential of 1.45 V, the current density decreased from 2.2 to 1.3 mA cm^{-2} during electrolysis for 15 h (ca. 60% of the current was retained; see Figure S14). We also examined the stability of films generated in different numbers of CV cycles (i.e. 1, 10, and 50 cycles). Our results showed that for films formed in one CV cycle, the current rapidly decreased from 1.9 to less than 0.3 mA cm^{-2}, whereas for films formed in 10 and 50 cycles, more than 70% of the current could be retained. At higher applied potentials, the generation of O_2 bubbles became more violent, which caused the catalyst film to fall from the ITO electrode (see Table S2). As the amount of catalyst deposited in a few CV cycles was small, catalyst loss and thus current decrease are striking. However, more of the catalyst was deposited in 50 CV cycles, which caused the influence of catalyst loss on the current to be less marked (i.e. more of the catalyst was stored as a backup).[44]

The Tafel plot of this iron-based film was determined in 0.1 M phosphate buffer (pH 7.0) at different applied potentials. All data were collected with iR compensation. Stable currents were measured at applied potentials ranging from 1.21 to 1.35 V at every 20 mV step for 600 s CPE experiments with stirring. A steady state could be obtained at every particular potential with currents ranging from 3.1 μA cm^{-2} to 1.37 mA cm^{-2}. The Tafel plot of η versus log$j$ produced a slope of 52 mV per decade (Figure 3c), which further indicated the outstanding activity of this iron-based film for electrocatalytic water oxidation.

In summary, iron-based films were prepared as highly active WOCs by a fast and simple electrodeposition method. The film can be generated in less than a minute in several cycles of CV from dilute Fe^{II} in a neutral acetate buffer. These conditions are critical to minimize time and energy costs for large-scale applications. The extremely low catalyst loading of 10.2 nmol of iron per 1.0 cm^2 of an ITO electrode is significant in improving atom efficiency and making the electrode transparent. The resultant film on GC and ITO electrodes can catalyze the electrochemical oxidation of water to O_2 from a phosphate buffer (pH 7.0) with a large current and moderate overpotentials. In a 20 h CPE experiment at 1.35 V and pH 7.0, an impressive TON of 1.5×10^4 and TOF of 756 h^{-1} for evolved oxygen per deposited Fe ion on ITO were observed. The use of iron, the fast and simple preparation method, the large current and TOF, the evolution of oxygen in neutral aqueous media, the transparency of the catalyst, and the high catalyst stability are remarkable. This study may therefore lead to more convenient and competitive routes for the conversion and usage of solar energy.

Keywords: electrocatalysis · film preparation · iron · oxygen evolution · water splitting

How to cite: *Angew. Chem. Int. Ed.* **2015**, *54*, 4870–4875
Angew. Chem. **2015**, *127*, 4952–4957

[1] T. R. Cook, D. K. Dogutan, S. Y. Reece, Y. Surendranath, T. S. Teets, D. G. Nocera, *Chem. Rev.* **2010**, *110*, 6474–6502.
[2] M. W. Kanan, D. G. Nocera, *Science* **2008**, *321*, 1072–1075.
[3] L. Cheng, W. J. Huang, Q. F. Gong, C. H. Liu, Z. Liu, Y. G. Li, H. J. Dai, *Angew. Chem. Int. Ed.* **2014**, *53*, 7860–7863; *Angew. Chem.* **2014**, *126*, 7994–7997.
[4] M. Dincă, Y. Surendranath, D. G. Nocera, *Proc. Natl. Acad. Sci. USA* **2010**, *107*, 10337–10341.
[5] S. M. Barnett, K. I. Goldberg, J. M. Mayer, *Nat. Chem.* **2012**, *4*, 498–502.
[6] M. R. Gao, W. C. Sheng, Z. B. Zhuang, Q. R. Fang, S. Gu, J. Jiang, Y. S. Yan, *J. Am. Chem. Soc.* **2014**, *136*, 7077–7084.
[7] R. Cao, W. Z. Lai, P. W. Du, *Energy Environ. Sci.* **2012**, *5*, 8134–8157.
[8] J. J. Concepcion, J. W. Jurss, M. K. Brennaman, P. G. Hoertz, A. O. T. Patrocinio, N. Y. M. Iha, J. L. Templeton, T. J. Meyer, *Acc. Chem. Res.* **2009**, *42*, 1954–1965.
[9] L. L. Duan, F. Bozoglian, S. Mandal, B. Stewart, T. Privalov, A. Llobet, L. C. Sun, *Nat. Chem.* **2012**, *4*, 418–423.
[10] Y. Lee, J. Suntivich, K. J. May, E. E. Perry, Y. Shao-Horn, *J. Phys. Chem. Lett.* **2012**, *3*, 399–404.
[11] R. Cao, H. Y. Ma, Y. V. Geletii, K. I. Hardcastle, C. L. Hill, *Inorg. Chem.* **2009**, *48*, 5596–5598.
[12] N. D. McDaniel, F. J. Coughlin, L. L. Tinker, S. Bernhard, *J. Am. Chem. Soc.* **2008**, *130*, 210–217.
[13] M. P. Santoni, G. La Ganga, V. M. Nardo, M. Natali, F. Puntoriero, F. Scandola, S. Campagna, *J. Am. Chem. Soc.* **2014**, *136*, 8189–8192.
[14] Y. Shimazaki, T. Nagano, H. Takesue, B. H. Ye, F. Tani, Y. Naruta, *Angew. Chem. Int. Ed.* **2004**, *43*, 98–100; *Angew. Chem.* **2004**, *116*, 100–102.
[15] I. Zaharieva, P. Chernev, M. Risch, K. Klingan, M. Kohlhoff, A. Fischer, H. Dau, *Energy Environ. Sci.* **2012**, *5*, 7081–7089.
[16] A. Yamaguchi, R. Inuzuka, T. Takashima, T. Hayashi, K. Hashimoto, R. Nakamura, *Nat. Commun.* **2014**, *5*, 4256.
[17] K. Jin, J. Park, J. Lee, K. D. Yang, G. K. Pradhan, U. Sim, D. Jeong, H. L. Jang, S. Park, D. Kim, N. E. Sung, S. H. Kim, S. Han, K. T. Nam, *J. Am. Chem. Soc.* **2014**, *136*, 7435–7443.
[18] J. Park, H. Kim, K. Jin, B. J. Lee, Y. S. Park, H. Kim, I. Park, K. D. Yang, H. Y. Jeong, J. Kim, K. T. Hong, H. W. Jang, K. Kang, K. T. Nam, *J. Am. Chem. Soc.* **2014**, *136*, 4201–4211.
[19] T. Takashima, K. Hashimoto, R. Nakamura, *J. Am. Chem. Soc.* **2012**, *134*, 18153–18156.
[20] A. Ramírez, P. Hillebrand, D. Stellmach, M. M. May, P. Bogdanoff, S. Fiechter, *J. Phys. Chem. C* **2014**, *118*, 14073–14081.

[21] J. L. Fillol, Z. Codolà, I. Garcia-Bosch, L. Gómez, J. J. Pla, M. Costas, *Nat. Chem.* **2011**, *3*, 807 – 813.
[22] D. K. Bora, A. Braun, E. C. Constable, *Energy Environ. Sci.* **2013**, *6*, 407 – 425.
[23] K. Jun, Y. S. Lee, T. Buonassisi, J. M. Jacobson, *Angew. Chem. Int. Ed.* **2012**, *51*, 423 – 427; *Angew. Chem.* **2012**, *124*, 438 – 442.
[24] G. Chen, L. J. Chen, S. M. Ng, W. L. Man, T. C. Lau, *Angew. Chem. Int. Ed.* **2013**, *52*, 1789 – 1791; *Angew. Chem.* **2013**, *125*, 1833 – 1835.
[25] M. K. Coggins, M.-T. Zhang, A. K. Vannucci, C. J. Dares, T. J. Meyer, *J. Am. Chem. Soc.* **2014**, *136*, 5531 – 5534.
[26] Y. Y. Liang, Y. G. Li, H. L. Wang, J. G. Zhou, J. Wang, T. Regier, H. J. Dai, *Nat. Mater.* **2011**, *10*, 780 – 786.
[27] S. Cobo, J. Heidkamp, P. A. Jacques, J. Fize, V. Fourmond, L. Guetaz, B. Jousselme, V. Ivanova, H. Dau, S. Palacin, M. Fontecave, V. Artero, *Nat. Mater.* **2012**, *11*, 802 – 807.
[28] G. P. Gardner, Y. B. Go, D. M. Robinson, P. F. Smith, J. Hadermann, A. Abakumov, M. Greenblatt, G. C. Dismukes, *Angew. Chem. Int. Ed.* **2012**, *51*, 1616 – 1619; *Angew. Chem.* **2012**, *124*, 1648 – 1651.
[29] D. K. Bediako, C. Costentin, E. C. Jones, D. G. Nocera, J. M. Savéant, *J. Am. Chem. Soc.* **2013**, *135*, 10492 – 10502.
[30] H. T. Lei, A. L. Han, F. W. Li, M. N. Zhang, Y. Z. Han, P. W. Du, W. Z. Lai, R. Cao, *Phys. Chem. Chem. Phys.* **2014**, *16*, 1883 – 1893.
[31] D. K. Bediako, B. Lassalle-Kaiser, Y. Surendranath, J. Yano, V. K. Yachandra, D. G. Nocera, *J. Am. Chem. Soc.* **2012**, *134*, 6801 – 6809.
[32] A. Singh, S. L. Y. Chang, R. K. Hocking, U. Bach, L. Spiccia, *Energy Environ. Sci.* **2013**, *6*, 579 – 586.
[33] M.-T. Zhang, Z. F. Chen, P. Kang, T. J. Meyer, *J. Am. Chem. Soc.* **2013**, *135*, 2048 – 2051.
[34] Z. F. Chen, T. J. Meyer, *Angew. Chem. Int. Ed.* **2013**, *52*, 700 – 703; *Angew. Chem.* **2013**, *125*, 728 – 731.
[35] R. D. L. Smith, M. S. Prévot, R. D. Fagan, Z. P. Zhang, P. A. Sedach, M. K. J. Siu, S. Trudel, C. P. Berlinguette, *Science* **2013**, *340*, 60 – 63.
[36] M. W. Louie, A. T. Bell, *J. Am. Chem. Soc.* **2013**, *135*, 12329 – 12337.
[37] S. Chen, J. J. Duan, M. Jaroniec, S. Z. Qiao, *Angew. Chem. Int. Ed.* **2013**, *52*, 13567 – 13570; *Angew. Chem.* **2013**, *125*, 13812 – 13815.
[38] L. Trotochaud, S. L. Young, J. K. Ranney, S. W. Boettcher, *J. Am. Chem. Soc.* **2014**, *136*, 6744 – 6753.
[39] J. Y. C. Chen, J. T. Miller, J. B. Gerken, S. S. Stahl, *Energy Environ. Sci.* **2014**, *7*, 1382 – 1386.
[40] E. Y. Tshuva, S. J. Lippard, *Chem. Rev.* **2004**, *104*, 987 – 1011.
[41] I. G. Denisov, T. M. Makris, S. G. Sligar, I. Schlichting, *Chem. Rev.* **2005**, *105*, 2253 – 2277.
[42] T. M. Garakani, P. Norouzi, M. Hamzehloo, M. R. Ganjali, *Int. J. Electrochem. Sci.* **2012**, *7*, 857 – 874.
[43] D. M. Soolaman, H. Z. Yu, *J. Phys. Chem. C* **2007**, *111*, 14157 – 14164.
[44] Y. Surendranath, M. W. Kanan, D. G. Nocera, *J. Am. Chem. Soc.* **2010**, *132*, 16501 – 16509.
[45] A. P. Grosvenor, B. A. Kobe, M. C. Biesinger, N. S. McIntyre, *Surf. Interface Anal.* **2004**, *36*, 1564 – 1574.
[46] N. S. McIntyre, D. G. Zetaruk, *Anal. Chem.* **1977**, *49*, 1521 – 1529.
[47] V. Spanu, C. N. Turcanu, *J. Radioanal. Nucl. Chem.* **1994**, *181*, 189 – 200.
[48] M. L. Sun, G. Rousse, A. M. Abakumov, G. Van Tendeloo, M. T. Sougrati, M. Courty, M. L. Doublet, J. M. Tarascon, *J. Am. Chem. Soc.* **2014**, *136*, 12658 – 12666.
[49] W. D. Chemelewski, H. C. Lee, J. F. Lin, A. J. Bard, C. B. Mullins, *J. Am. Chem. Soc.* **2014**, *136*, 2843 – 2850.
[50] M.-K. Liang, M. J. Limo, A. Sola-Rabada, M. J. Roe, C. C. Perry, *Chem. Mater.* **2014**, *26*, 4119 – 4129.
[51] Z. F. Chen, A. R. Rathmell, S. R. Ye, A. R. Wilson, B. J. Wiley, *Angew. Chem. Int. Ed.* **2013**, *52*, 13708 – 13711; *Angew. Chem.* **2013**, *125*, 13953 – 13956.
[52] M. Fekete, R. K. Hocking, S. L. Y. Chang, C. Italiano, A. F. Patti, F. Arena, L. Spiccia, *Energy Environ. Sci.* **2013**, *6*, 2222 – 2232.
[53] J. F. Moulder, W. F. Stickle, P. E. Sobol, K. D. Bomben, *Handbook of X-ray Photoelectron Spectroscopy*, PerkinElmer, Eden Prairie, **1992**.
[54] P. Nagaraju, C. Srilakshmi, N. Pasha, N. Lingaiah, I. Suryanarayana, P. S. S. Prasad, *Appl. Catal. A* **2008**, *334*, 10 – 19.
[55] D. H. Yu, C. Wu, Y. Kong, N. H. Xue, X. F. Guo, W. P. Ding, *J. Phys. Chem. C* **2007**, *111*, 14394 – 14399.

Received: December 25, 2014
Revised: February 9, 2015
Published online: February 27, 2015

